Article

Proinflammatory Signaling Regulates Hematopoietic Stem Cell Emergence

Raquel Espín-Palazón,[1,2] David L. Stachura,[1,4] Clyde A. Campbell,[1] Diana García-Moreno,[2] Natasha Del Cid,[1] Albert D. Kim,[1] Sergio Candel,[2] José Meseguer,[2] Victoriano Mulero,[2,*] and David Traver[1,3,*]

[1]Department of Cellular and Molecular Medicine, University of California, San Diego, 9500 Gilman Drive, Natural Sciences Building 6107, La Jolla, CA 92093, USA
[2]Departamento de Biología Celular e Histología, Facultad de Biología, Universidad de Murcia, IMIB-Arrixaca, Campus Universitario de Espinardo, Murcia 30100, Spain
[3]Section of Cell and Developmental Biology, University of California, San Diego, La Jolla, CA 92093, USA
[4]Present address: Department of Biological Sciences, California State University, 400 West First Street, Chico 95929-0515 CA, USA
*Correspondence: vmulero@um.es (V.M.), dtraver@ucsd.edu (D.T.)
 http://dx.doi.org/10.1016/j.cell.2014.10.031

SUMMARY

Hematopoietic stem cells (HSCs) underlie the production of blood and immune cells for the lifetime of an organism. In vertebrate embryos, HSCs arise from the unique transdifferentiation of hemogenic endothelium comprising the floor of the dorsal aorta during a brief developmental window. To date, this process has not been replicated in vitro from pluripotent precursors, partly because the full complement of required signaling inputs remains to be determined. Here, we show that TNFR2 via TNFα activates the Notch and NF-κB signaling pathways to establish HSC fate, indicating a requirement for inflammatory signaling in HSC generation. We determine that primitive neutrophils are the major source of TNFα, assigning a role for transient innate immune cells in establishing the HSC program. These results demonstrate that proinflammatory signaling, in the absence of infection, is utilized by the developing embryo to generate the lineal precursors of the adult hematopoietic system.

INTRODUCTION

In all vertebrate animals studied, the homeostasis of adult blood and immune cells is ultimately maintained by rare subsets of hematopoietic stem cells (HSCs) (Kondo et al., 2003). During a brief window during embryonic development, these HSCs arise de novo from hemogenic endothelium comprising the floor of the dorsal aorta (DA) (Bertrand et al., 2010a; Boisset et al., 2010; de Bruijn et al., 2000; Kissa and Herbomel, 2010) in a process that appears to be conserved among all vertebrates (Clements and Traver, 2013; Godin and Cumano, 2002). A more complete understanding of the signaling pathways that instruct HSC emergence could in principle inform in vitro approaches utilizing pluripotent precursors to create patient-specific HSCs (Kyba and Daley, 2003). Despite decades of efforts, this goal has not yet been achieved, in part due to an incomplete understanding of the native molecular cues needed to establish HSC fate.

One known requirement for HSC emergence is signaling through the Notch pathway (Bigas et al., 2013). Notch regulates many forms of intercellular communication, underlying many cell-fate decisions, including key roles in embryonic patterning (Kopan and Ilagan, 2009). Although the role of Notch in the maintenance and function of adult HSCs appears to be dispensable (Bigas and Espinosa, 2012), Notch signaling is absolutely required in the embryonic specification of HSCs in both the mouse (Bigas and Espinosa, 2012) and zebrafish (Bertrand et al., 2010b). In mice, the Notch receptor Notch1 (Kumano et al., 2003) and the Notch ligand Jagged1 (Jag1) are required for HSC specification (Bigas et al., 2010). It is important to note that, because Notch signaling is also indispensable for arterial specification (Quillien et al., 2014) and because HSCs derive directly from the aortic floor, it has been difficult to distinguish whether Notch signaling regulates HSC emergence independently from its role in upstream arterial specification. Recent studies in Jag1-deficient mice have demonstrated HSC defects in the presence of normal arterial development, suggesting that these Notch requirements may be distinct and separable. Recent studies have also demonstrated that Notch signaling is required intrinsically within HSCs or their precursors (Robert-Moreno et al., 2008) via function of the Notch1 receptor (Hadland et al., 2004), suggesting that Jag1 may be a specific ligand of Notch1 in the specification of HSCs.

Tumor necrosis factor α (TNFα) is a powerful proinflammatory cytokine that plays a pivotal role in the regulation of inflammation and immunity. TNFα exerts its functions via engagement of one of two specific cell surface receptors (TNFRs), namely the 55 kDa TNFR1 (also known as TNFRSF1A) and the 75 kDa TNFR2 (also known as TNFRSF1B) (Shalaby et al., 1990). TNFR1 is expressed in most cell types, whereas TNFR2 is restricted to immune and endothelial cells (Aggarwal, 2003). Whereas TNFα signaling regulates aspects of adult hematopoiesis (Mizrahi and Askenasy, 2014), a potential role in the developmental specification of HSCs has not been addressed. However, it has been reported that TNFα and its receptors are highly expressed in the murine yolk sac and fetal liver, suggesting a possible role for this inflammatory cytokine in embryonic hematopoiesis (Kohchi et al., 1994).

Nuclear factor-kappa B (NF-κB) is a ubiquitous, inducible transcription factor that is activated by a diverse number of stimuli, including TNFα (Ahn and Aggarwal, 2005; Brown et al., 2008). A

Cell
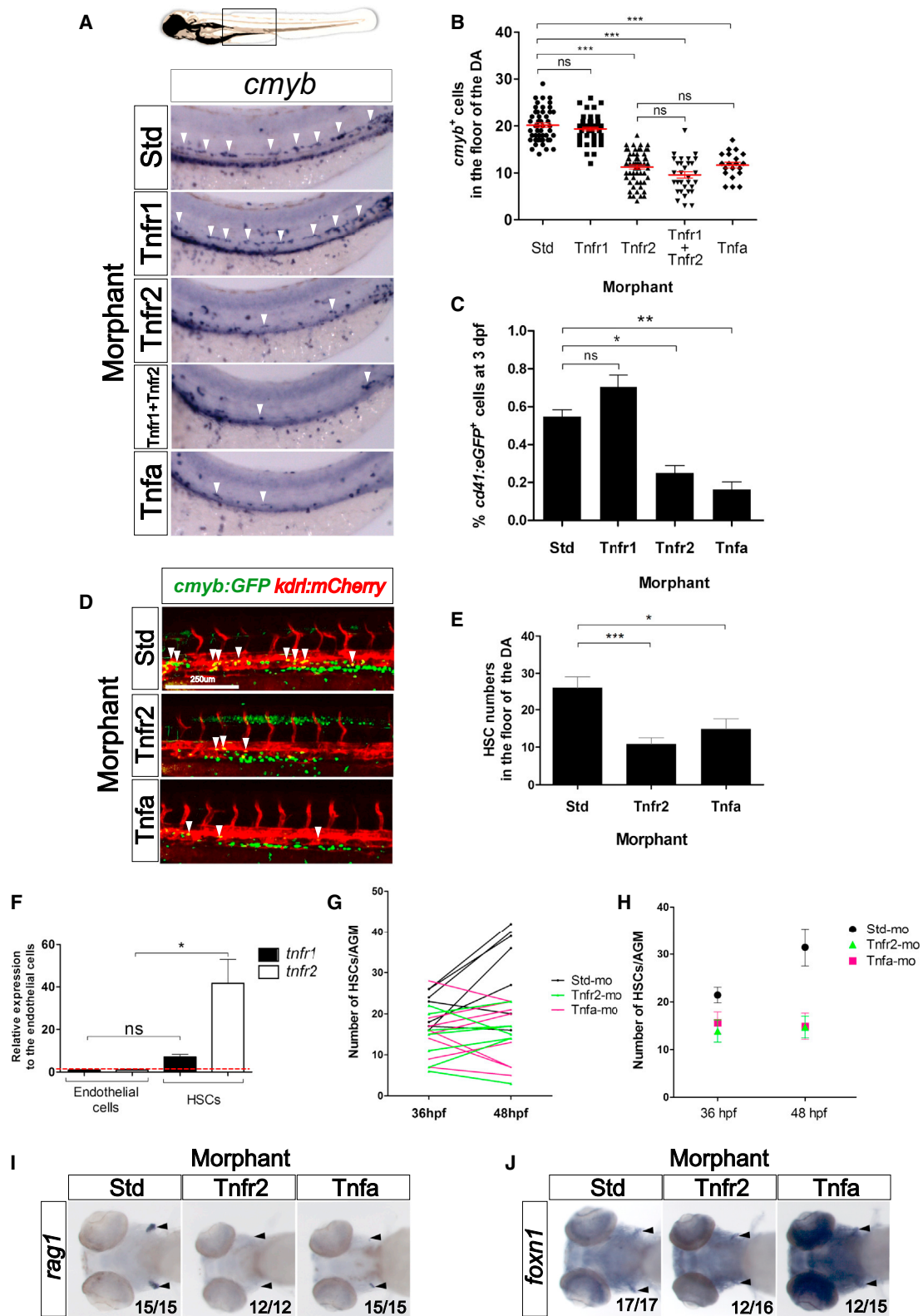
Figure 1. Tnfa and Tnfr2 Are Required for HSC Generation

(A) Standard control (Std), Tnfr1, Tnfr2, Tnfa, Tnfr1, and Tnfr2 morphants were examined by WISH for *cmyb* expression in the aortic floor at 48 hpf. White arrowheads denote *cmyb*[+] HSPCs.

(legend continued on next page)

multitude of downstream targets, as well as upstream inducers, position NF-κB as a general sensor of cell stress. TNFα signaling through TNFR2 is a well-known activator of NF-κB (Aggarwal et al., 2012; Faustman and Davis, 2010). TNFα activates NF-κB through its canonical pathway, in which IκBs (NF-κB inhibitors) are phosphorylated, ubiquitinated, and degraded, releasing NF-κB dimers that then translocate to the nucleus to bind specific NF-κB DNA binding sites to activate gene expression (Brown et al., 2008). A direct role of NF-κB in HSCs has not been extensively studied, although recent reports indicate that NF-κB positively regulates the transcription of genes involved in the maintenance and homeostasis of hematopoietic stem and progenitor cells (HSPCs) (Stein and Baldwin, 2013), as well as their microenvironmental interactions (Zhao et al., 2012). Whether or not NF-κB is important in HSC emergence has not been investigated.

TNFα and TNFRs (Tnfa and Tnfrs utilizing zebrafish nomenclature) are well conserved in all vertebrate organisms (Wiens and Glenney, 2011), and we previously demonstrated that zebrafish Tnfa interacts with Tnfr1 and Tnfr2 (Espín et al., 2013). Recent studies in the zebrafish indicate that zebrafish Tnfa functions as a proinflammatory cytokine by activating endothelial cells (Roca et al., 2008). Additionally, the genetic inhibition of Tnfrs identified an essential role for Tnfa signaling in the development and maintenance of endothelial cells (Espín et al., 2013). Because HSCs arise from hemogenic endothelial cells, we queried whether TNF signaling plays a role in HSC emergence. In the present study, we demonstrate a previously unappreciated requirement for TNF signaling in the generation of HSCs. We also show that NF-κB is active in nascent HSCs and that this activation is essential for HSC emergence. Finally, we identify primitive neutrophils as a key source of Tnfa, assigning these cells a previously unidentified role in HSC development. In summary, we report an important role for inflammatory signaling in the birth of the adult hematopoietic system that is mediated by the proinflammatory cytokine Tnfa, the inflammatory transcription factor NF-κB, and the Notch signaling pathway under nonpathogenic conditions.

RESULTS

Tnfa Signaling through Tnfr2 Is Required for Definitive, but Not Primitive, Hematopoiesis

We previously demonstrated that Tnfa is required for embryonic blood vessel development (Espín et al., 2013). Because HSCs are generated from arterial vessels in the embryo (Bigas et al., 2013), we investigated whether this proinflammatory cytokine also played a role in HSC development. To address this question, we isolated $kdrl^+$ endothelial cells by fluorescence-activated cell sorting (FACS) from 26 hr postfertilization (hpf) transgenic $kdrl:mCherry$ embryos and performed quantitative PCR (qPCR) for $tnfr1$ and $tnfr2$. Both transcripts were enriched in these cells compared to the whole embryo (Figure S1A available online). Sorted cells expressed high levels of endogenous $kdrl$ and were negative for the muscle-specific $myod$ gene, demonstrating the purity of the sorted cells (Figure S1B). To investigate whether Tnfa signaling was required for HSC specification, we performed loss-of-function experiments for Tnfa and its two receptors, Tnfr1 and Tnfr2, utilizing specific antisense morpholinos (MOs) (Espín et al., 2013). In the zebrafish embryo, HSCs can be visualized along the axial vessels by expression of $cmyb$ using whole-mount in situ hybridization (WISH) (Burns et al., 2005). The number of $cmyb^+$ cells in or near the floor of the DA was significantly reduced in Tnfa- and Tnfr2-deficient embryos compared with their wild-type (WT) siblings (Figures 1A and 1B). However, loss of Tnfr1 showed no effect on HSC number, and its simultaneous depletion with Tnfr2 was not significantly different than loss of Tnfr2 alone (Figures 1A and 1B), indicating that the action of Tnfa through Tnfr2, but not Tnfr1, is important in HSC development. This result was supported by quantitation of $cd41:eGFP^+$ HSPCs (Bertrand et al., 2008) using flow cytometry, which were significantly decreased in Tnfr2- and Tnfa- deficient fish at 3 days postfertilization (dpf) (Figure 1C).

To further confirm the reduction of HSCs in Tnfr2- and Tnfa-deficient embryos, we directly visualized emerging HSCs from the floor of the DA in $kdrl:mCherry; cmyb:GFP$ double transgenic embryos (Bertrand et al., 2010a) at 48 hpf by confocal microscopy (Figure 1D). Consistent with the results above, the number of double-positive $kdrl^+; cmyb^+$ HSCs in the floor of the DA was reduced ∼50% when compared to control embryos (Figures 1D and 1E), unaffected in Tnfr1 deficient embryos, and showed a similar 50% decrease in Tnfr1+Tnfr2 double-depleted embryos (Figure S1C). These reductions could be due to a defect in the initial specification of HSCs or in their subsequent maintenance. To distinguish between these possibilities, we performed WISH for the nascent HSC marker $runx1$ at earlier time points. Both Tnfr2- and Tnfa- deficient embryos showed significant reduction in the number of $runx1^+$ cells in the aortic floor at 24,

(B) Quantification of $cmyb^+$ HSPCs from (A). Each dot represents total $cmyb^+$ cells per embryo. The mean ± SEM for each group of embryos is shown in red.

(C) $cd41:eGFP$ transgenic embryos were injected with Std, Tnfr1, Tnfr2, and Tnfa MOs and subjected to flow cytometric analysis at 3 dpf. Each bar represents the percentage of $cd41$:GFP$^+$ cells in each sample and is the mean ± SEM of three to seven independent samples of five embryos each.

(D) Maximum projections of 48 hpf $cmyb:GFP; kdrl:mCherry$ double-transgenic embryos injected with Std, Tnfr2, and Tnfa MOs. Arrowheads denote $cmyb^+$, $kdrl^+$ HSCs along the DA. All views: anterior to left.

(E) Enumeration of $cmyb^+$, $kdrl^+$ HSCs shown in (D). Bars represent mean ± SEM of Std (n = 13), Tnfr2 (n = 13), and Tnfa (n = 8) morphants.

(F) $cmyb^-$, $kdrl^+$ endothelial cells and $cmyb^-$, $kdrl^+$ HSCs were isolated from $cmyb:GFP; kdrl:mCherry$ transgenic fish by FACS at 48 hpf and examined for expression of $tnfr1$ and $tnfr2$. Bars represent mean ± SEM of two biological replicates.

(G) Confocal tracking of HSC numbers in the floor of the DA from individual $cmyb:GFP; kdrl:mCherry$ transgenic animals at 36 and 48 hpf following depletion of Tnfr2 or Tnfa compared to standard control morphants.

(H) Means ± SEM of $cmyb^+$ cell numbers from (G).

(I and J) WISH for the T lymphocyte and thymic epithelial markers $rag1$ (I) and $foxn1$ (J) (black arrowheads), respectively, in Tnfr2 and Tnfa morphants compared to Std controls at 4 dpf. All views are ventral, with anteriors to left. Numbers represent embryos with displayed phenotype; ns, not significant; *p < 0.05, **p < 0.01, and ***p < 0.001.

See also Figure S1.

Cell

28, and 36 hpf (Figures S1D and S1E), indicating that the functions of Tnfa and Tnfr2 are important during the earliest steps of HSC specification.

We next examined subsequent developmental stages for possible roles of Tnfa in the maintenance of nascent HSCs. To determine whether Tnf receptor expression is modulated following HSC specification, we purified $kdrl^+; cmyb^-$ endothelial cells and $kdrl^+; cmyb^+$ HSCs from 48 hpf $kdrl:mCherry; cmyb: GFP$ embryos by FACS. qPCR analysis showed that, whereas $tnfr1$ mRNA levels were similar in HSCs and endothelial cells, $tnfr2$ transcripts markedly increased in HSCs (Figure 1F). As this result suggested that Tnfr2 may play a role in HSC maintenance, we analyzed changes in HSC number in individual embryos over time. The number of $cmyb^+; kdrl^+$ cells in WT animals expanded between 36 and 48 hpf, whereas Tnfr2- or Tnfa-deficient siblings showed similar numbers of HSCs at either time point (Figures 1G and 1H). Together, these results suggest that Tnfa signaling through Tnfr2 is important both in the first steps of HSC specification and in their subsequent maintenance following emergence from the aortic endothelium. Finally, we examined later larval stages by monitoring the expression of $rag1$ and lck, two genes expressed in developing thymocytes (Langenau et al., 2004) because the T cell lineage derives exclusively from HSCs (Bertrand et al., 2008; Gering and Patient, 2005). Expression of $rag1$ was completely or nearly absent, respectively, in Tnfr2- and Tnfa-deficient animals at 4 dpf (Figure 1I). However, the thymic anlage developed normally in all morphants, assessed by the expression of the thymic epithelial marker $foxn1$ (Figure 1J). These results were further verified utilizing $lck:eGFP$ transgenic animals to track T cell development (Langenau et al., 2004). T cells were absent in Tnfr2- and Tnfa- deficient larvae at 4 dpf, whereas Tnfr1-deficient siblings showed normal T cell development (Figure S1F). Together, these results indicate that Tnfa signals via Tnfr2 and that this signaling pathway is important both for early specification and subsequent maintenance of HSC fate, such that the lineage is apparently lost by 4 dpf.

To further dissect the role of Tnfa signaling in hematopoiesis, we assessed whether Tnfa and its receptors were required for the first waves of hematopoiesis, commonly referred to as "primitive" due to the transience of these cells and lack of upstream multipotent progenitors. In zebrafish, primitive hematopoiesis generates macrophages, neutrophils, and erythrocytes. The expression of $csf1ra$, a specific marker of macrophages (Herbomel et al., 2001), was unaffected in Tnfa-, Tnfr1-, and Tnfr2-deficient embryos at 24 hpf (Figure S1G). Additionally, primitive neutrophils were unaffected at 30 hpf, as assayed using transgenic $mpx:eGFP$ animals (data not shown). Similarly, primitive erythropoiesis, assessed by expression of the erythroid-specific transcription factor $gata1a$ at 24 hpf, was unaffected in morphant embryos (Figure S1G). Overall, these results indicate that Tnfa signaling is dispensable for primitive hematopoiesis and indispensable for definitive hematopoiesis in the zebrafish embryo.

Tnfr2- and Tnfa-Deficient Embryos Display Normal Vasculogenesis

Because HSCs originate in arterial vessels, many mutants with vascular or arterial specification defects also have hematopoie-

tic defects (Bigas and Espinosa, 2012). No vascular abnormalities were observed in Tnfr2- or Tnfa-deficient embryos at 24 hpf when assayed by WISH for the endothelial marker $kdrl$ at the MO doses used in this study (Figure 2A), and circulation was normal ($gata1:DsRed^+$, red blood cells) but reduced numbers of HSPCs and thrombocytes ($cd41:eGFP^+$) at 3 dpf (Figure 2B). These results suggest that the functions of Tnfr2 and Tnfa are required specifically during HSC development independently of their role in developing vasculature. Thus, we could uncouple the vascular defects previously described for Tnfr2 (Espín et al., 2013) from its effects on HSC development using lower doses of Tnfr2 MO.

To address whether HSC defects in Tnfr2- and Tnfa-deficient animals were a consequence of impaired arterial specification, we performed WISH for the arterial markers $efnb2a$, dlc, $notch1b$, and $notch3$ (Lawson et al., 2001) in morphant embryos at 28 hpf. We observed no alterations in transcript levels when compared to control siblings (Figure 2C). Taken together, these data indicate that Tnfa signaling through Tnfr2 is specifically required for HSC development.

### Tnfr2 Is Intrinsically Required for HSC Development

Because Tnfr2 is expressed in endothelial cells (Figure S1A), we hypothesized that Tnfr2 is intrinsically required within the vascular lineage for HSC development. To test this hypothesis, we generated a transgenic zebrafish line in which the WT form of $tnfr2$ is upregulated via induction of the Gal4 transcriptional transactivator. HSC development was observed by confocal microscopy following overexpression of Tnfr2 specifically within the vasculature in $fli1a:Gal4; UAS:RFP; cmyb:GFP; UAS:tnfr2$ animals. The number of RFP$^+$GFP$^+$ HSCs in quadruple transgenic embryos was significantly increased compared to their Tnfr2$^-$ siblings (Figures 2D and 2E), demonstrating that Tnfr2 activity induces or supports the HSC program following targeted expression to the vasculature.

To verify that the loss of HSCs in Tnfr2 morphants was not due to the apoptosis of endothelial cells, we performed a TUNEL assay and immunohistochemistry for GFP in $kdrl:GFP$ embryos injected with Tnfr2 MO. Analysis of endothelial cells by confocal microscopy at 28 hpf indicated that loss of Tnfr2 caused no increased apoptotic endothelial cells within the DA (Figure S2A), even though there was an increase in apoptotic nonendothelial cells. As a positive control for apoptosis in control animals, we imaged the lens of the eye (Cole and Ross, 2001) (Figure S2B). We also performed WISH for $runx1$ in the same experiment to verify the reduction of HSCs in these embryos (Figures S2C and S2D). These results, together with the findings that there are no detectable apoptotic endothelial cells in the DA at 28 hpf (Kobayashi et al., 2014) indicate that the HSC specification defect in Tnfr2-deficient embryos is not caused by apoptosis induced by alterations of Tnfr1/Tnfr2 ratios within the vasculature.

### Tnfa Signaling Acts Upstream of Notch during HSC Specification

During Notch activation, Notch receptors are stimulated by ligands from neighboring cells, triggering the cleavage of the Notch intracellular domain (NICD), which enters the nucleus to
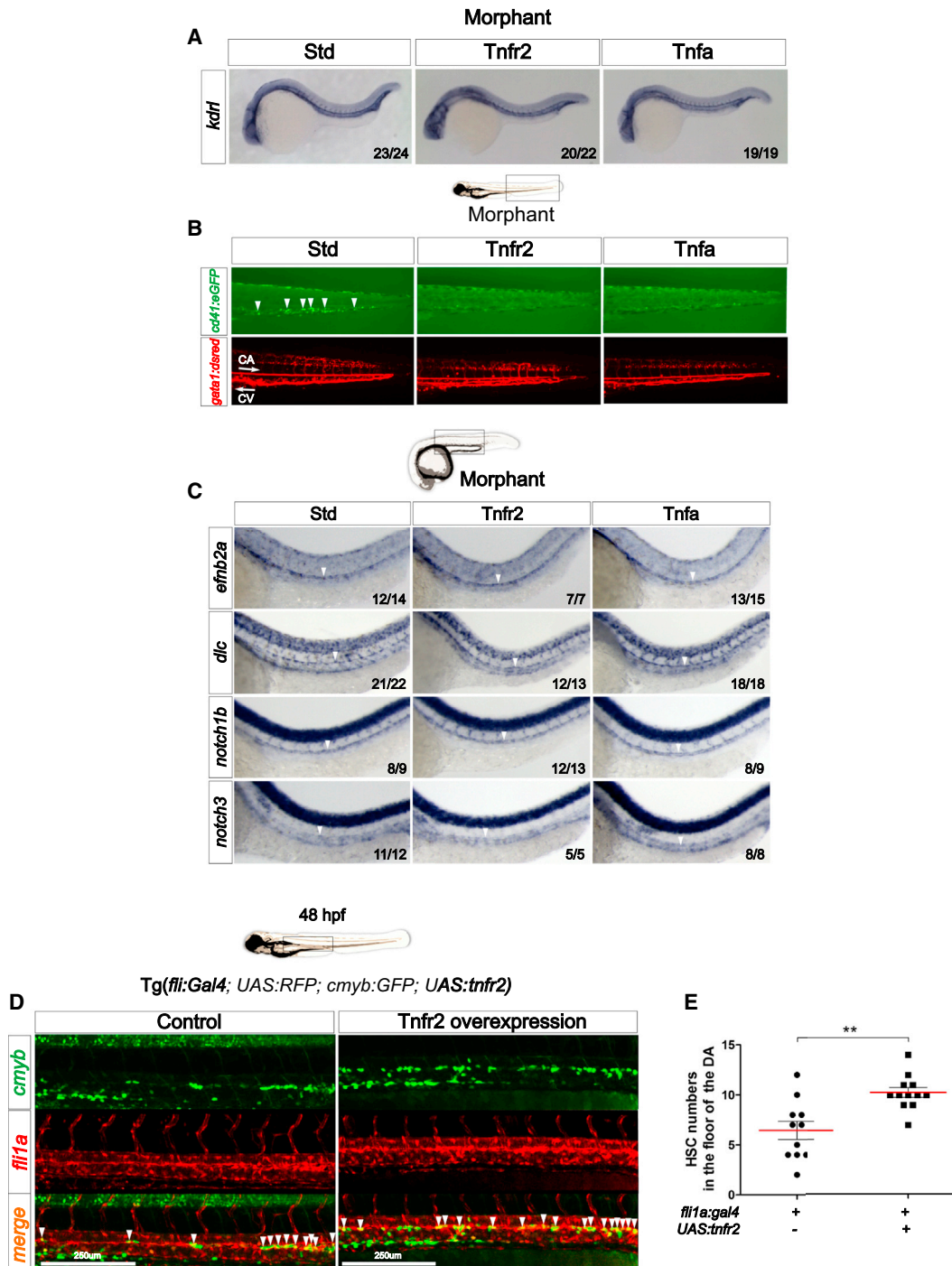
Figure 2. Signaling through Tnfr2 Regulates HSC Development Independently of Its Role in Vascular Formation

(A) Std, Tnfr2, and Tnfa morphants were interrogated by WISH for the expression of *kdrl* at 24 hpf.

(B) *cd41*:eGFP*; gata1a*:dsred double-transgenic embryos were injected with Std, Tnfr2, and Tnfa MOs and visualized at 3 dpf. Arrowheads indicate *cd41*:GFP$^+$ HSPCs in the CHT located between the caudal artery (CA) and caudal vein (CV). Arrows indicate blood flow direction.

(C) Expression of the arterial markers *efnb2a*, *dlc*, *notch1b*, and *notch3* in Std, Tnfr2, and Tnfa morphants analyzed by WISH at 28 hpf. Arrowheads denote the CA.

(D) Maximum projections of *fli1a:Gal4; UAS:tnfr2; cmyb:GFP; kdrl:mCherry* transgenic embryos at 48 hpf. Region shown includes the DA, and arrowheads denote *cmyb*$^+$; *kdrl*$^+$ HSCs.

(E) Enumeration of *cmyb*$^+$; *kdrl*$^+$ HSCs shown in (D). Each dot is the number of *kdrl*$^+$; *cmyb*$^+$ cells per embryo. Means ± SEM for each group is shown in red. **p < 0.01. All views are lateral, with anteriors to the left. Numbers in panels represent larvae with indicated phenotype.

See also Figure S2.
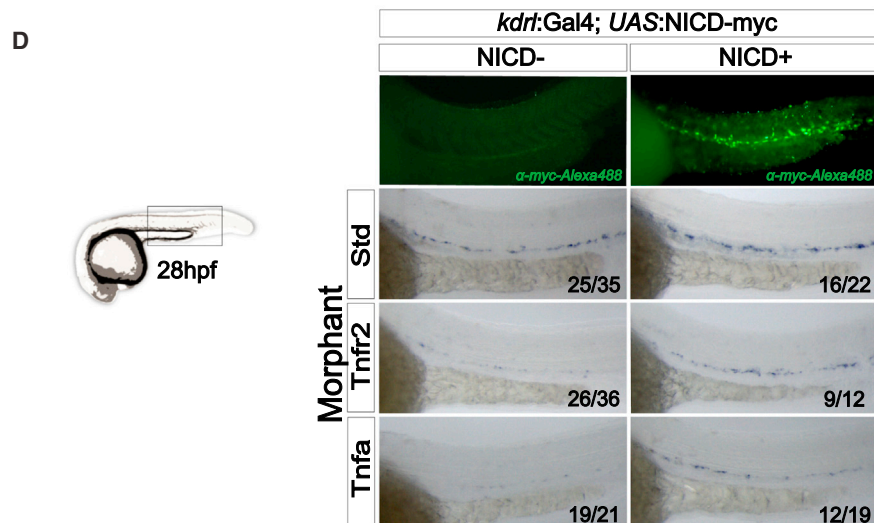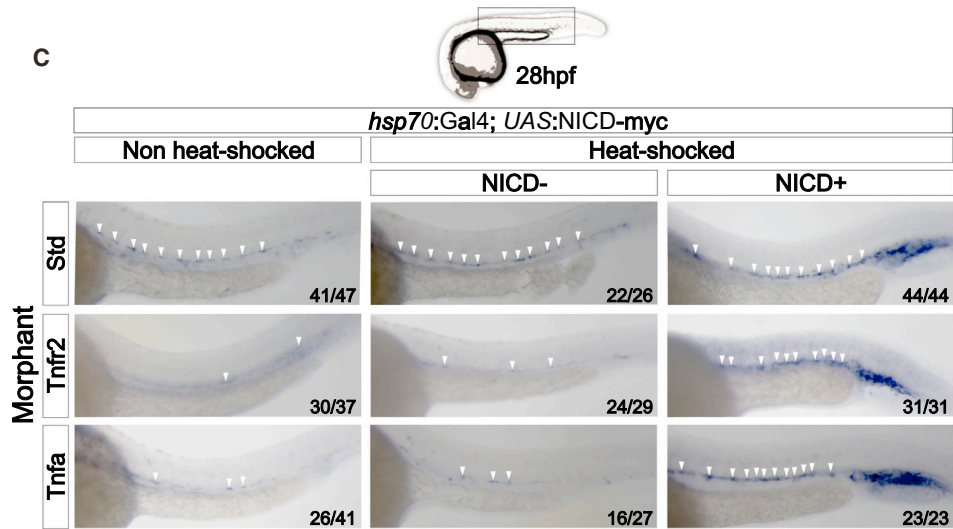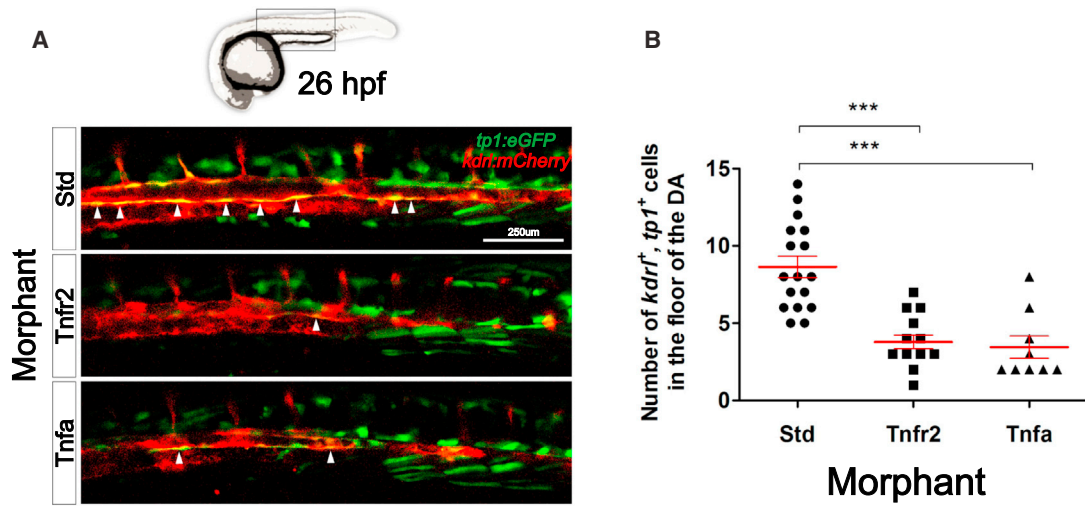
(legend on next page)

Cell

function as transcription factor essential for cell fate decisions (Lai, 2004). There are four Notch receptors (Notch1a, 1b, 2, and 3), five Delta family ligands (Dla, Dlb, Dlc, Dld, and Dll4) and three Jagged ligands (Jagged 1a, Jagged 1b, and Jagged 2) in zebrafish. Because TNFα activates the Notch pathway in certain contexts (Fernandez et al., 2008; Wang et al., 2013), we queried whether signaling through Tnfr2 may similarly activate Notch signaling to specify HSCs. We performed loss-of-function experiments for Tnfr2 and Tnfa in transgenic *tp1:eGFP* animals, in which GFP is expressed by cells having recently experienced Notch signaling (Parsons et al., 2009). Consistent with our other findings, the depletion of either Tnfa or Tnfr2 led to a 2-fold reduction in *tp1:eGFP+; kdrl:mCherry+* HSPCs in the aortic floor at 26 hpf (Figure 3A, arrowheads, and Figure 3B). These observations indicate that Tnfr2 signaling is upstream of Notch signaling during HSC specification.

If Notch signaling is indeed required downstream of Tnfr2 function for HSC specification, then ectopic expression of the Notch1a intracellular domain (NICD1a) should rescue the lack of HSCs in Tnfr2- and Tnfa-deficient embryos. We performed two different experiments to address the timing and tissue specificity of this Tnfa-dependent Notch requirement. To provide temporal control of NICD1a induction, we utilized inducible *hsp70:Gal4; UAS:NICD1a-myc* double-transgenic embryos, which express NICD1a under the control of the inducible Gal4 system. Induction of NICD1a at 18 hpf rescued the depletion of *runx1+* HSCs at 28 hpf along the DA in both Tnfa and Tnfr2 morphants (Figure 3C). We then enforced the expression of NICD1a within endothelial cells utilizing *kdrl:Gal4; UAS:NICD1a-myc* double-transgenic embryos that had been injected with Tnfr2 or Tnfa MOs. Endothelial expression of NICD1a restored *runx1+* cells along the aortic floor (Figure 3D), indicating that TNF signaling activates the Notch pathway within hemogenic endothelium to specify HSC fate.

Tnfa Induces Jag1a within Endothelial Cells to Promote HSC Specification through Notch1a

We next investigated potential mechanisms by which Tnfa and Tnfr2 induced Notch activation. Due to the fact that Tnfa signaling has been reported to induce or inhibit the expression of specific Notch ligands (Fernandez et al., 2008; Sainson et al., 2008), we analyzed expression of the eight zebrafish Notch ligands within purified *kdrl+* endothelial cells from Tnfr2-deficient embryos. Only *jag1a* expression was downregulated in Tnfr2 morphants relative to controls (Figure 4A). Using a *fli1a:Gal4* driver to enforce expression of Tnfr2 specifically within the vasculature, we examined Notch ligand expression in *fli1a:Gal4; UAS:tnfr2* animals by qPCR (Figure 4B). We detected a 20-fold increase of *tnfr2* in *UAS:tnfr2+* compared to *UAS:tnfr2−* embryos

(Figure 4B). Consistent with our previous results, only *jag1a* mRNA levels were increased following the enforced expression of Tnfr2 (Figure 4B).

Interestingly, Jag1 is required for the generation of definitive hematopoietic cells in mice but is dispensable for arterial development. A potential role for Jag1 in zebrafish HSPC development has not been addressed. Two paralogues of the single *JAG1* human gene are present in the zebrafish genome: *jag1a* and *jag1b*. Because only *jag1a* levels were modulated by Tnfr2, we performed loss-of-function experiments with this gene. Loss of *jag1a* led to decreased HSC numbers as analyzed by *runx1* expression along the DA (Figure 4C). However, specification of aortic fate was normal, as *efnb2a* and *dlc* levels were unperturbed (Figure 4C). To further verify that Tnfr2 and Jag1a were in the same genetic pathway, we performed synergy studies by coinjecting low doses of Tnfr2 and Jag1a MOs simultaneously. Aortic *runx1+* cells were significantly reduced in Tnfr2- and Jag1a- double-deficient embryos compared to single-deficient embryos (Figure 4D). Tnfr2 function thus lies genetically upstream of *jag1a* during HSC specification. To investigate potential Jag1a-presenting cells, we isolated *cmyb−, kdrl+* endothelial cells and *cmyb+, kdrl+* HSCs for qPCR analysis of *jag1a* at 48 hpf. *jag1a* transcripts were 4-fold more abundant in endothelial cells than in HSCs (Figure S3), suggesting that Notch signaling in HSCs or hemogenic endothelium is activated by neighboring Jag1a+ endothelial cells.

We next investigated which of the four Notch receptors were downstream of Jag1a during HSC induction. In the mouse, Notch1 is required within HSCs or their lineal precursors to instruct HSC fate. We therefore focused upon the two zebrafish orthologs of human NOTCH1, Notch1a and Notch1b. To investigate whether either receptor functioned downstream of Tnfr2 to specify HSCs, we performed synergy experiments by coinjecting low doses of Tnfr2 MO with morpholinos against Notch1a or Notch1b. Only the simultaneous depletion of Tnfr2 and Notch1a, but not Tnfr2 and Notch1b, led to a statistically significant decrease in *runx1* expression compared to single morphants at 28 hpf (Figure 4E). This finding suggests that Notch1a serves as the Notch receptor for Jag1a to specify HSC fate downstream of Tnfr2.

The Proinflammatory Transcription Factor NF-κB Is Active in Emerging HSCs

Activation of TNF receptors by ligand binding leads to the recruitment of adaptor proteins that trigger NF-κB activation (Aggarwal et al., 2012). Moreover, the induction of *Jag1* transcription by Tnfa in murine endothelial cells is NF-κB dependent (Johnston et al., 2009). Interestingly, NF-κB (as well as Tnfr2 and Jag1) is necessary for embryonic vessel development (Santoro et al., 2007). These lines of evidence suggested that NF-κB could

---

Figure 3. Tnfa and Tnfr2 Act Upstream of Notch Signaling during HSC Specification

(A) *tp1:eGFP; kdrl:mCherry* embryos injected with Std, Tnfr2, and Tnfa MOs were visualized at 26 hpf. Arrowheads indicate cells in the floor of the DA with active Notch signaling.

(B) Enumeration of *tp1+, kdrl+* HSCs from (A). Each dot represents the number of HSCs per embryo, and red lines indicate means ± SEM. ***p < 0.001.

(C) *hsp70:Gal4; UAS:NICD-myc* embryos injected with Std, Tnfr2, and Tnfa MOs were heat shocked at 18 hpf and WISH for *runx1* was performed at 28 hpf. Arrowheads denote HSCs along the DA.

(D) *kdrl:Gal4; UAS:NICD-myc* embryos injected with Std, Tnfr2, and Tnfa MOs were analyzed by WISH for *runx1* at 28 hpf. NICD+ larvae were identified using anti-myc-Alexa488 antibody (top). Numbers in panels represent the numbers of larvae with indicated phenotype.
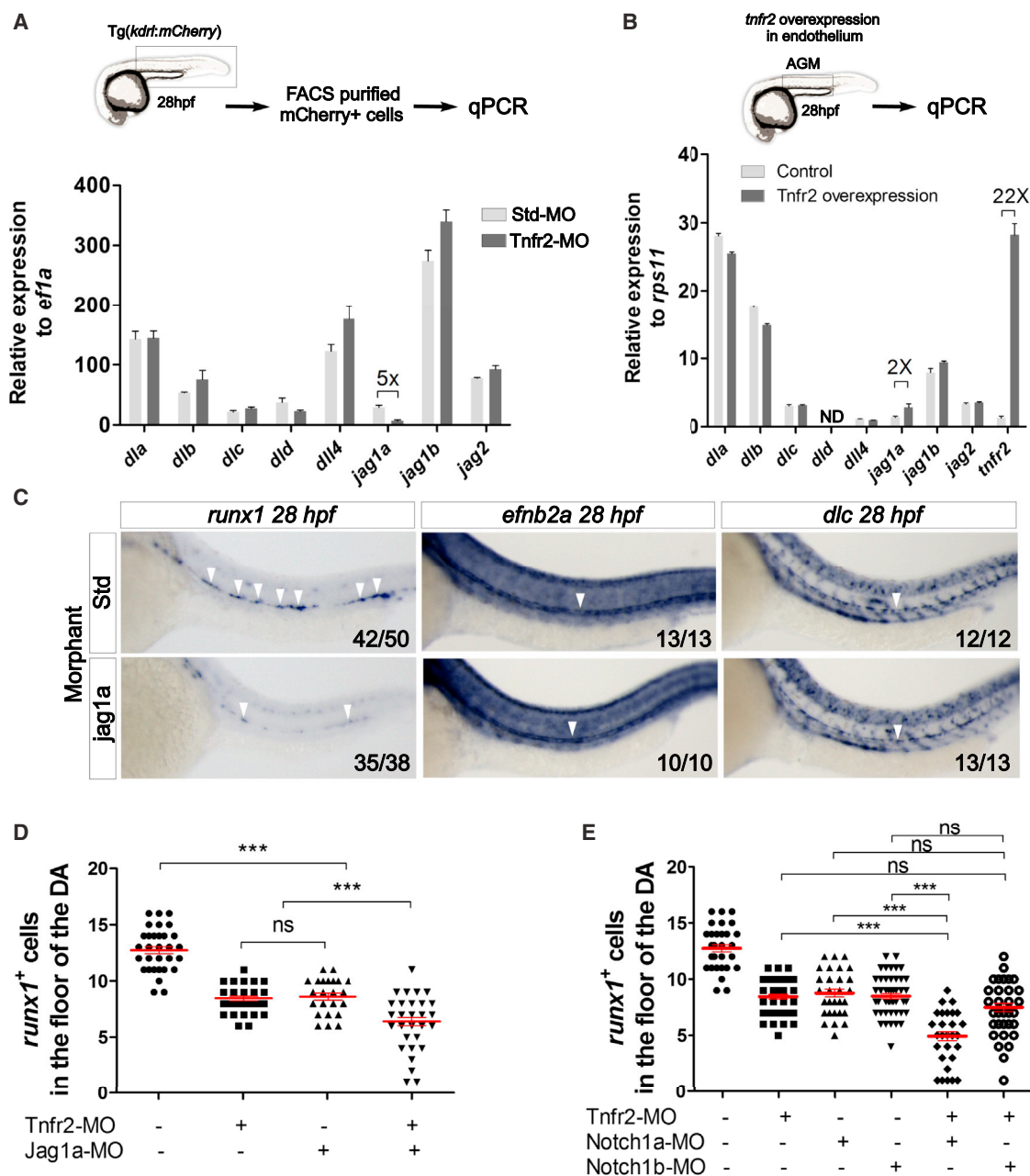
Cell

Figure 4. Tnfr2 Induces *jagged1a* in Endothelial Cells, Encouraging HSC Specification

(A) *kdrl:mCherry*^{+} cells from dissected trunks of Std or Tnfr2 morphants were purified by FACS at 28 hpf for qPCR. Levels of indicated transcripts along x axis are shown relative to the housekeeping gene *ef1a*. Bars represent means ± SEM of duplicate samples.

(B) AGM regions from *fli1a:Gal4; UAS:tnfr2* embryos were dissected and subjected to qPCR for transcripts shown along x axis. Bars represent means ± SEM of triplicate samples expression relative to the housekeeping gene *rps11*.

(C) Std (top) or Jag1a (bottom) morphants were interrogated for *runx1* expression at 26 hpf and *efnb2a* and *dlc* at 28 hpf by WISH. Numbers represent larvae with indicated phenotype.

(D) Enumeration of *runx1*^{+} cells in Tnfr2 and/or Jag1a morphants at 28 hpf.

(E) Enumeration of *runx1*^{+} cells in Tnfr2 and/or Notch1a and/or Notch1b morphants at 28 hpf. Each dot is the number of HSCs per embryo, and red lines indicate means ± SEM (D and E) ***p < 0.001; ns, not significant.

See also Figure S3.

have a previously unappreciated role in HSC specification, prompting us to examine its role in HSC development. We utilized an NF-κB activation reporter transgenic line (Kanther et al., 2011) in combination with the *kdrl:mCherry* transgene to perform confocal analysis of the DA at different time points. Interestingly, we observed NF-κB^{high} cells in the floor of the DA at

Cell

24 hpf, typically in pairs and in direct contact with each other (Figure 5A). We also observed *NF-κB+* cells along the roof of the DA but at a much lower frequency than in the floor (data not shown). *NF-κB+, kdrl+* cells remained visible at 30 hpf (Figure 5A) and underwent endothelial-to-hematopoietic transition (EHT) (Movie S1), a characteristic feature of emerging HSCs. To further evaluate whether HSCs had increased NF-κB activation compared to their surrounding endothelial neighbors, *kdrl+; cmyb+* HSCs and *kdrl+; cmyb−* endothelial cells were isolated from 48 hpf *kdrl:mCherry; cmyb:GFP* embryos by FACS for qPCR analyses. Whereas endothelial cells had 20- to 30-fold induction of the NF-κB response genes interleukin 1 beta (*il1b*) and nuclear factor of kappa light polypeptide gene enhancer in B cells inhibitor alpha a (*ikbaa*) relative to whole-embryo expression, HSCs displayed 300- and 2,300-fold increases in *il1b* and *ikbaa*, respectively (Figure 5B). Immunohistochemistry for the NF-κB subunit p65 in *kdrl:mCherry* embryos showed that, although p65 was detected in the cytoplasm of every cell as expected, it was more intense in the pronephros (Figures 5C and 5D, yellow asterisks), in the DA, and in cells potentially undergoing the endothelial to hematopoietic transition in the aortic floor (Figures 5C and 5D, arrow). These results indicate that NF-κB activation is a characteristic feature of emerging HSCs.

Multiple lines of evidence support the integration of the Notch and NF-κB signaling pathways during the differentiation of various cell types (Ang and Tergaonkar, 2007; Cao et al., 2011; Espinosa et al., 2010; Espinosa et al., 2003; Shin et al., 2006; Song et al., 2008). For this reason, we investigated whether *NF-κB+* cells in the floor of the DA also had active Notch signaling, utilizing double-transgenic *tp1:nlsCherry; NFKB:GFP* animals to simultaneously visualize respective Notch and NF-κB activation. *NF-κB+* cells in the floor of the DA were also *tp1+* (Figure 5E). No *NF-κB+, tp1−* cells were found in the floor of the DA, suggesting that Notch is (or was previously) active in *NF-κB+* HSPCs.

NF-κB Activation Is Required for HSC Specification and Acts Downstream of Tnfr2

To determine whether NF-κB function is required for HSC emergence, we developed a Tg(*UAS:dn-ikbaa*) transgenic animal that functions as a dominant-negative inhibitor of NF-κB (Figures S4A and S4B). Similar truncation constructs have been utilized in vitro to inhibit NF-κB activation (Abbas and Abu-Amer, 2003). At 6 hr post-heat-shock in *hsp70:Gal4; UAS:dn-ikbaa* animals, *dn-ikbaa* mRNA levels were detected in *dn-ikbaa+*, but not in *dn-ikbaa−*, siblings (Figure S4C). qPCR for the NF-κB response gene *il1b* in FACS-purified *fli1a+* endothelial cells showed significant downregulation in the *dn-ikbaa+* embryos compared to their *dn-ikbaa−* siblings (Figures S4D and S4E). Lipopolysaccharide (LPS) challenge of WT embryos produced a significant increase in *il1b* expression compared to PBS-injected controls, as previously described (van der Vaart et al., 2013), but not in *dn-ikbaa+* embryos (Figures S4F and S4G), indicating that *dn-ikbaa+* embryos are unable to trigger an inflammatory response through NF-κB. These results thus demonstrate that *UAS:dn-ikbaa* embryos have impaired NF-κB activation.

Blockade of NF-κB function at 20 hpf in *hsp70:Gal4; UAS:dn-ikbaa* animals led to loss of HSCs at 48 hpf (Figure 6A). Loss of NF-κB specifically within the vasculature using *fli1a:Gal4; UAS:dn-ikbaa* double-transgenic embryos also led to a depletion of *cmyb+* cells (Figure 6B). qPCR for *il1b* in FACS-purified endothelial cells showed a 3-fold decrease in Tnfr2 morphants (Figure 6C), demonstrating that NF-κB acts downstream of Tnfr2 during HSC specification. Together, these results suggest that NF-kB activation in hemogenic endothelium is a key event in the specification of HSCs.

Primitive Neutrophils Are the Key Source of Tnfa

In adult organisms, immune cells are the main source of TNFα, including T and B lymphocytes, macrophages, and neutrophils (Aggarwal, 2003). From 22 to 72 hpf, the temporal window over which zebrafish HSCs emerge from aortic endothelium, the only leukocytes present are primitive myeloid cells, namely macrophages and neutrophils (Herbomel et al., 1999; Le Guyader et al., 2008). Interestingly, *tnfa* expression in the zebrafish embryo was not detectable during the first 9 hr of development but was expressed before 24 hpf (Espín et al., 2013) when HSCs are initially specified (Clements and Traver, 2013). We therefore hypothesized that primitive myeloid cells were the source of Tnfa. We isolated *mpeg:GFP+* primitive macrophages and *mpx:GFP+* primitive neutrophils by FACS at two different time points and performed qPCR for *tnfa* (Figure 7A). Although both populations expressed *tnfa*, the highest expression was observed within the neutrophil fraction (Figure 7A). We then utilized a pu1 MO to specifically ablate both primitive myeloid lineages in vivo (Rhodes et al., 2005). pu1 MO efficacy was validated by WISH using the panleukocyte marker *l-plastin* and the neutrophil marker *mpx* at 48 hpf (Figure S5A). Following ablation of primitive myeloid cells in pu1 morphants, HSCs were enumerated by confocal microscopy of *kdrl+cmyb+* cells. A 2-fold decrease in HSC number was detected in pu1 morphants compared to their control siblings (Figures 7B and 7C). To elucidate which primitive myeloid population was responsible for the decrease in HSC number, we utilized an irf8 MO (Li et al., 2011), which skews myeloid development to almost entirely neutrophilic. Loss of the macrophage lineage was confirmed in irf8 morphants by qPCR for the macrophage-specific marker *mpeg1* (Figure S5B). Surprisingly, the number of *kdrl+; cmyb+* HSCs increased following loss of the macrophage lineage (Figures 7D and 7E). In agreement with our *tnfa* expression data, this result suggests that neutrophils are the key source of the Tnfa needed for HSC emergence. To test this hypothesis, we quantified *tnfa* expression levels in pu1- and irf8-deficient animals. Expression of *tnfa* was consistently decreased following loss of pu1 function and increased following loss of irf8 function (Figure 7F). In addition, although *runx1* was upregulated in irf8-deficient embryos, the simultaneous depletion of Tnfa and Irf8 led to a marked reduction in *runx1* expression, despite the elevated numbers of neutrophils present (Figure 7G). These findings demonstrate that production of Tnfa from primitive neutrophils is critical for the specification and/or maintenance of HSC fate.

Overall, these data indicate that production of Tnfa from primitive neutrophils activates Tnfr2, upregulating the expression of Jag1a on the surface of endothelial cells. Jag1a in turn activates Notch1a, triggering a signaling cascade whereby NF-κB triggers

Cell
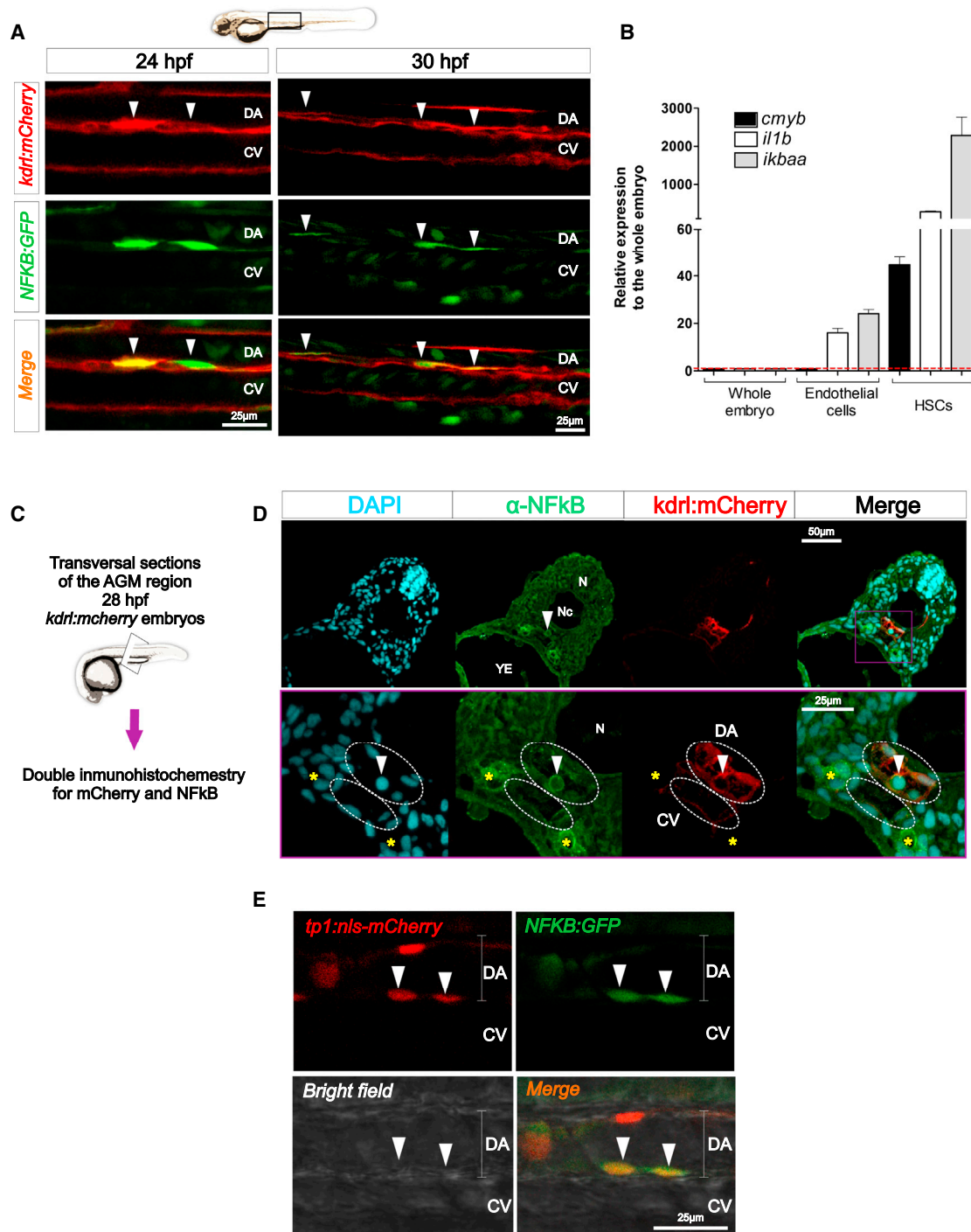
Figure 5. NF-κB Is Active in Emerging HSCs

(A) Trunk region of *kdrl:mCherry; NFKB:GFP* double-transgenic animals visualized by confocal microscopy at 24 hpf (left) and 30 hpf (right). Each image is a 2 μm z slice. Arrowheads denote HSCs.

(B) $cmyb^-$, $kdrl^+$ endothelial cells and $cmyb^+$, $kdrl^+$ HSCs were isolated by FACS at 48 hpf. Levels of the NF-κB target genes *ikbaa* and *il1b*, as well as the HSC marker *cmyb*, are shown relative to *ef1a*. Bars represent means ± SEM of two biological replicates.

(C) Schematic representation of the experimental design of (D). 28 hpf *kdrl:mCherry* animals were transversally sectioned and subjected to double immuno-histochemistry for mCherry (red) and NF-κB (green). DAPI (blue) was added to visualize nuclei.

(legend continued on next page)

Cell
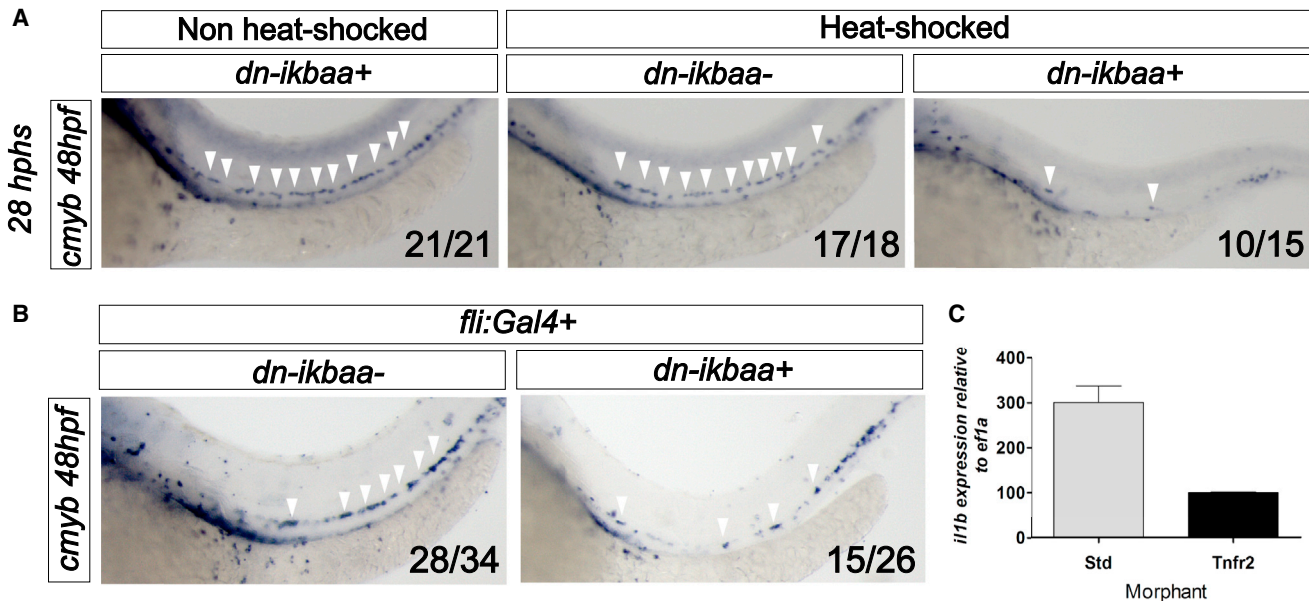
Figure 6. NF-κB Is Required for HSC Specification and Acts Downstream of Tnfr2

(A) hsp70:Gal4; UAS:dn-ikbaa embryos were heat shocked at 20 hpf. WISH for cmyb was performed at 48 hpf.

(B) WISH for cmyb in fli1a:Gal4; UAS:dn-ikbaa⁻ (left) and fli1a:Gal4; UAS:dn-ikbaa⁺ (right) embryos. Arrowheads mark cmyb⁺ cells along the DA.

(C) kdrl:mCherry⁺ cells were FACS sorted from Std or Tnfr2 morphants at 28 hpf for qPCR. Levels of the NF-κB target gene il1b are shown relative to ef1a. Bars represent means ± SEM from duplicate samples.

See also Figure S4.

a transcriptional program required for the emergence of HSCs from hemogenic endothelium (Figures S5C and S5D).

DISCUSSION

Traditionally, infection and inflammation were thought to play an indirect role in HSC homeostasis by causing increased proliferation and skewed differentiation toward microbicidal immune cell lineages (Takizawa et al., 2012). However, recent studies indicate that HSCs can respond directly to the inflammatory cytokines interferon (IFN) α/β, γ, and TNFα (Baldridge et al., 2011; King and Goodell, 2011). Additionally, there is evidence that HSCs can upregulate cytokines under stress-induced hematopoiesis (Zhao et al., 2014). Here, we examined a much earlier step in the biology of HSCs—their specification and emergence from hemogenic endothelium in the developing embryo. The emergence of HSCs from the aortic floor is transient and occurs during developmental windows when the surrounding environment is relatively sterile, whether it is in utero in mammals or within the chorion in teleosts. It is therefore surprising that a key pathway underlying the canonical response to infection and inflammation is required to generate the founders of the adult hematopoietic system. Our studies in the zebrafish demonstrate that depletion of Tnfa or its cognate receptor Tnfr2 leads to depletion of emerging HSCs. The key event elaborated by Tnfr2 appears to be activation of the Notch pathway because ectopic provision of Notch signaling rescued HSCs in the absence of Tnfa or Tnfr2 function. Although Notch signaling is required for HSC specification across vertebrate phyla, little is known regarding how this Notch event is regulated or which of the many receptors or ligands are necessary to fate HSCs from ventral aortic endothelium.

That the HSC program can be rescued in either Tnfa or Tnfr2 morphants by enforced expression of NICD1a within the vasculature demonstrates that the TNF pathway lies upstream of Notch in HSC specification. Our results suggest that signaling via Tnfr2 specifically controls Notch activation by inducing the Notch ligand jag1a in cells within the DA. Synergy experiments depleting Notch1a and Tnfr2 combinatorially indicate that Notch1a is likely the receptor on HSCs that binds to the Jag1a ligand presented by aortic endothelial cells. These findings are consistent with studies in the mouse embryo, where Notch1 is required cell autonomously within HSCs or their lineal precursors for their specification (Hadland et al., 2004; Kumano et al., 2003). The zebrafish Notch1a and Notch1b receptors are evolutionary paralogues of mammalian Notch1 (Kortschak et al., 2001) and

(D) Maximum projections of 1 μm sections. Arrowhead indicates a potential HSC emerging in the DA. DA and CV are demarcated by dashed white lines. Yellow asterisks indicate pronephric ducts.

(E) tp1:nls-mCherry; NFKB:GFP animals were visualized by confocal microscopy at 24 hpf. Each image is a 2 μm z slice. Arrowheads indicate HSCs. CV, caudal vein; DA, dorsal aorta; N, neural tube; Nc, notochord; YE, yolk extension.

See also Movie S1.
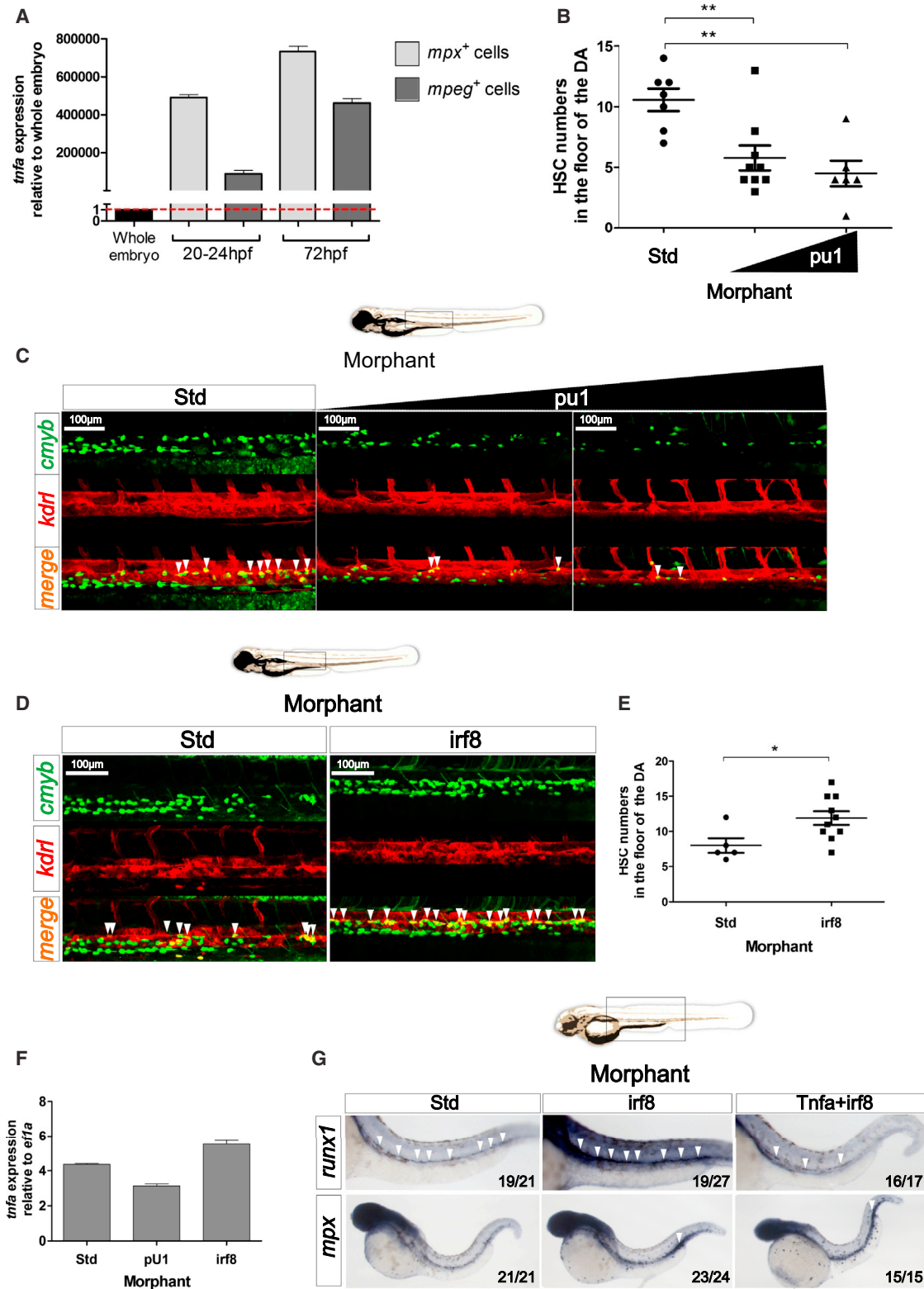
Cell

Figure 7. Primitive Myeloid Cells Play a Key Role in HSC Specification

(A) Primitive neutrophils (*mpx:GFP*[+]) and macrophages (*mpeg:GFP*[+]) were isolated at 20–24 and 72 hpf by FACS and *tnfa* expression was quantified by qPCR. Expression was normalized to *ef1a* and is presented relative to whole-embryo expression. Bars represent means ± SEM of two independent experiments.

(legend continued on next page)

Cell

are both expressed in the DA during the window of HSC emergence (Quillien et al., 2014). Our findings extend these results by demonstrating that Notch1 function is evolutionarily conserved in the specification of HSCs and provide a more detailed mechanism regarding how Notch1 may actually function in this process. Further studies will be required to determine the precise interactions between Jag1a and Notch1a and how these interactions lead to establishment of HSC fate.

In addition to its regulation of the Notch pathway, our results also suggest that Tnfa exerts its effects through NF-κB. Although NF-κB is known to play a key role in adult mammalian hematopoiesis (Gerondakis et al., 2012), a role in the embryonic emergence of HSCs has not been reported. The utilization of a *NFκB:GFP* reporter line allowed us to image the in vivo activation of NF-κB, indicating that this activation is required within endothelial cells of the DA for HSC emergence. Furthermore, these studies suggest that this activity is downstream of Tnfa/Tnfr2 signaling. Intriguingly, these data also demonstrate that NF-κB⁺ cells in the floor of the DA are often positive for Notch activity when assessed along with the *tp1* Notch reporter line. Whereas recent evidence suggests that Notch1 can modulate NF-κB activity in different cellular contexts, it remains to be determined whether one factor is epistatic to the other or if both may operate together within the hemogenic endothelium to establish HSC fate.

In this study, we have also discovered an unexpected role for neutrophils in HSC development. Whereas macrophages are involved in a broad array of developmental processes (Wynn et al., 2013), an active role for neutrophils in modulating developmental events has not been described. Here, we report for the first time that primitive neutrophils are a major source of Tnfa and that the loss of either neutrophils or Tnfa results in the loss of developing HSCs. The prevailing view that primitive myeloid cells have evolved predominantly to provide early immunity is thus likely oversimplistic. At any time point during HSC emergence, whether early during HSC specification or later during EHT, we observed ∼2-fold decreases in HSC number. That the lineal descendants of HSCs, most importantly T lymphocytes, are absent by 4–5 dpf indicates that the Tnfa/Tnfr2 signaling axis is required to sustain HSC function. Collectively, our findings suggest that activation of Tnfr2 is important both in hemogenic endothelium and in maintaining nascent HSC fate. It is important to note that *tnfa* is also expressed in endothelial cells (data not shown); contribution from the endothelium may thus play a role in either or both of these processes. The means to create conditional, tissue-specific gene disruption in the zebrafish will be required to precisely address the relative importance of each source.

In conclusion, we show that TNFα, a cytokine that has become the paradigm for induction of inflammatory responses, is also key in the establishment of the hematopoietic system through its influence on HSC formation in the developing embryo. In addition to the known signaling inputs required to establish HSC fate, inflammatory signals should now be added to this list. A major challenge for the field is to integrate each of these required inputs to better understand their spatial and temporal requirements, such that this knowledge may be utilized to instruct HSC fate in vitro from human pluripotent precursors, a major unrealized goal of regenerative medicine.

EXPERIMENTAL PROCEDURES

Zebrafish Husbandry and Strains
Zebrafish embryos and adults were mated, staged, raised, and processed as described (Westerfield, 2000) and maintained in accordance with UCSD IACUC guidelines. See Extended Experimental Procedures for description of transgenic lines.

Heat-Shock Treatment
For induction of *hsp70l:Gal4*-driven transgenes, embryos were placed in E3 medium and transferred to a 38°C water bath for 45 min at noted stages.

Generation of Transgenic Animals
Tg (UAS:dnnfkbiaa)ˢᵈ³⁵ and *Tg(UAS:tnfr2)ᵘᵐˢ¹* embryos were generated by Tol2-mediated transgenesis via the multisite Gateway cloning system (Invitrogen). See also Extended Experimental Procedures.

Morpholino Injection
Specific antisense targeting MOs (Gene Tools) were resuspended in DEPC-treated water at 1–3 mM and injected in one-cell stage embryos. See also Extended Experimental Procedures.

Enumeration of HSCs
Animals were subjected to WISH for *runx1* and *cmyb* at noted stages, and positive cells were imaged and manually counted. Confocal microscopy was performed on *cmyb:GFP; kdrl:mCherry* double-transgenic animals (Bertrand et al., 2010a), *tp1:eGFP; kdrl:mCherry* double-transgenic animals, and *NF-κB:GFP; kdrl:mCherry* double-transgenic animals. Z sections of the DA region were captured on a Leica SP5 microscope (Leica) using Volocity Acquisition, Visualization, and Restoration software (Improvision) and were manually counted.

Fluorescent Visualization of Blood Flow, HSPCs, and T Cells
To visualize blood flow, HSPCs, and T cells, *cd41:eGFP; gata1:dsred* embryos at 3 dpf and *lck:GFP* larvae at 4 dpf, respectively, were anesthetized in Tricaine (200 μg/ml) and examined using a Leica MZ16FA stereomicroscope.

Flow Cytometry and FACS
Briefly, embryos were dechorionated with pronase, anesthetized in tricaine, and dissociated with liberase or triturated with a P1000 pipette. The resulting

---

(B) Enumeration of *cmyb*⁺; *kdrl*⁺ HSCs shown in (C). Each dot represents total *cmyb*⁺; *kdrl*⁺ cells per embryo, and black lines indicate means ± SEM for each group of embryos. **p<0.01.

(C) Maximum projections of representative images of *cmyb:GFP; kdrl:mCherry* embryos at 48 hpf following injections of Std or pu1 MOs, the latter at two different concentrations. Region shown is the DA, and arrowheads denote *cmyb*⁺; *kdrl*⁺ HSCs.

(D) Maximum projections of representative images of *cmyb:GFP; kdrl:mCherry* embryos at 48 hpf in Std and irf8 morphants. Arrowheads denote *cmyb*⁺; *kdrl*⁺ HSCs.

(E) Enumeration of *cmyb*⁺; *kdrl*⁺ HSCs shown in (D).

(F) *tnfa* expression relative to *ef1a* in 28 hpf Std, pu1, or irf8 morphants. Bars represent means ± SEM of duplicate samples.

(G) Std, irf8, and irf8+Tnfa morphants were interrogated by WISH for *runx1* and *mpx* at 28 hpf. All views are lateral, with anteriors to the left. Numbers represent larvae with indicated phenotypes. *p < 0.05 and ***p < 0.001.

See also Figure S5.

Cell

suspension was filtered with a 40 μm cell strainer, and flow cytometric acquisitions or FACS were performed on a FACS LSRII. See also Extended Experimental Procedures.

Whole-Mount RNA In Situ Hybridization

WISH was carried out as described (Thisse et al., 1993). Probes for the *gata1a*, *csfr1ra*, *kdrl*, *cmyb*, *runx1*, *foxn1*, *efnb2a*, *dlc*, *notch1b*, *notch3*, and *rag1* transcripts were generated using the DIG RNA Labeling Kit (Roche Applied Science) from linearized plasmids. *dn-ikbaa* probe was generated from bp 118-933 of *dn-IkBaa* (see Figure S2). Embryos were imaged using a Leica M165C stereomicroscope equipped with a DFC295 color digital camera (Leica) and FireCam software (Leica).

Statistical Analyses

Data were analyzed by analysis of variance (ANOVA). In all figures, solid red bars denote the mean, and error bars represent SEM. * $p < 0.05$, ** $p < 0.01$, and *** $p < 0.001$; n.s., not significant; n.d., not detected.

Quantitative RT-PCR Analysis

RNA was isolated from tissues with RNeasy (QIAGEN), and cDNA was generated with qScript Supermix (Quanta BioSciences). Primers to detect zebrafish transcripts are described in Table S1. Relative expression levels of genes were calculated by the following formula: relative expression = $2^{-(Ct[gene\ of\ interest]\ -Ct[housekeeping\ gene])}$.

Immunofluorescence of NICD⁺ Animals

The immunofluorescence staining for cMyc in *hsp70:gal4*; *UAS:NICD-myc* zebrafish embryos was performed as previously described (Kim et al., 2014).

Detection of Apoptotic Cell Death by TUNEL Labeling

The TUNEL assay was performed as previously described (Espín et al., 2013) with slight modifications. See also Extended Experimental Procedures.

Lipopolysaccharide Injections

Tg(*hsp:Gal4; UAS:dn-ikbaa*) embryos were manually dechorionated at 24 hpf, followed by heat shock at 38°C for 50 min. Four hr post-heat-shock, 2 nl of PBS or LPS (900 μg/ml) (L6511, Sigma) was injected into the posterior blood island (PBI). Embryos were then harvested 1 hr postinjection (hpi), and RNA was isolated for qPCR analysis.

Microtome Sections and Immunohistochemistry

Embryos were fixed with 4% PFA, embedded in paraffin, and sectioned at 5 μm in thickness with Leica microtome. Immunohistochemistry was performed as previously described (Kobayashi et al., 2014). The following antibodies were used: mouse anti-mCherry 1:500 (Abcam, ab125096), rabbit anti-p65 (NF-κB) (RB-1638-P; Lab Vision) 1:200, donkey anti-rabbit IgG Alexa Fluor 594-conjugated (Molecular Probes, A-21207) 1:1,000, and donkey anti-mouse IgG Alexa Fluor 488-conjugated (Molecular Probes, A-11029) in addition to DAPI 1:1000 (Life Technologies, D3571).

SUPPLEMENTAL INFORMATION

Supplemental Information includes Extended Experimental Procedures, five figures, one table, and one movie and can be found with this article online at http://dx.doi.org/10.1016/j.cell.2014.10.031.

AUTHOR CONTRIBUTIONS

All studies presented herein derive from initial observations by R.E.-P. in the laboratory of V.M. R.E.-P., D.L.S., C.A.C., N.D.C., A.D.K., J.M., D.T., and V.M. designed experiments; R.E.-P., D.L.S., C.A.C., D.G.-M., N.D.C., and S.C. performed research; R.E.-P., D.L.S., C.A.C., D.G-M., N.D.C., A.D.K., S.C., J.M., V.M., and D.T. analyzed data; and R.E.-P., D.L.S., V.M., and D.T. wrote the paper with minor contributions from the remaining authors.

REFERENCES

Abbas, S., and Abu-Amer, Y. (2003). Dominant-negative IkappaB facilitates apoptosis of osteoclasts by tumor necrosis factor-alpha. J. Biol. Chem. *278*, 20077–20082.

Aggarwal, B.B. (2003). Signalling pathways of the TNF superfamily: a double-edged sword. Nat. Rev. Immunol. *3*, 745–756.

Aggarwal, B.B., Gupta, S.C., and Kim, J.H. (2012). Historical perspectives on tumor necrosis factor and its superfamily: 25 years later, a golden journey. Blood *119*, 651–665.

Ahn, K.S., and Aggarwal, B.B. (2005). Transcription factor NF-kappaB: a sensor for smoke and stress signals. Ann. N Y Acad. Sci. *1056*, 218–233.

Ang, H.L., and Tergaonkar, V. (2007). Notch and NFkappaB signaling pathways: Do they collaborate in normal vertebrate brain development and function? Bioessays *29*, 1039–1047.

Baldridge, M.T., King, K.Y., and Goodell, M.A. (2011). Inflammatory signals regulate hematopoietic stem cells. Trends Immunol. *32*, 57–65.

Bertrand, J.Y., Kim, A.D., Teng, S., and Traver, D. (2008). CD41+ cmyb+ precursors colonize the zebrafish pronephros by a novel migration route to initiate adult hematopoiesis. Development *135*, 1853–1862.

Bertrand, J.Y., Chi, N.C., Santoso, B., Teng, S., Stainier, D.Y., and Traver, D. (2010a). Haematopoietic stem cells derive directly from aortic endothelium during development. Nature *464*, 108–111.

Bertrand, J.Y., Cisson, J.L., Stachura, D.L., and Traver, D. (2010b). Notch signaling distinguishes 2 waves of definitive hematopoiesis in the zebrafish embryo. Blood *115*, 2777–2783.

Bigas, A., and Espinosa, L. (2012). Hematopoietic stem cells: to be or Notch to be. Blood *119*, 3226–3235.

Bigas, A., Robert-Moreno, A., and Espinosa, L. (2010). The Notch pathway in the developing hematopoietic system. Int. J. Dev. Biol. *54*, 1175–1188.

Bigas, A., Guiu, J., and Gama-Norton, L. (2013). Notch and Wnt signaling in the emergence of hematopoietic stem cells. Blood Cells Mol. Dis. *51*, 264–270.

Boisset, J.C., van Cappellen, W., Andrieu-Soler, C., Galjart, N., Dzierzak, E., and Robin, C. (2010). In vivo imaging of haematopoietic cells emerging from the mouse aortic endothelium. Nature *464*, 116–120.

Brown, K.D., Claudio, E., and Siebenlist, U. (2008). The roles of the classical and alternative nuclear factor-kappaB pathways: potential implications for autoimmunity and rheumatoid arthritis. Arthritis Res. Ther. *10*, 212.

Burns, C.E., Traver, D., Mayhall, E., Shepard, J.L., and Zon, L.I. (2005). Hematopoietic stem cell fate is established by the Notch-Runx pathway. Genes Dev. *19*, 2331–2342.

Cao, Q., Kaur, C., Wu, C.Y., Lu, J., and Ling, E.A. (2011). Nuclear factor-kappa β regulates Notch signaling in production of proinflammatory cytokines and nitric oxide in murine BV-2 microglial cells. Neuroscience *192*, 140–154.

Clements, W.K., and Traver, D. (2013). Signalling pathways that control vertebrate haematopoietic stem cell specification. Nat. Rev. Immunol. 13, 336–348.

Cole, L.K., and Ross, L.S. (2001). Apoptosis in the developing zebrafish embryo. Dev. Biol. 240, 123–142.

de Bruijn, M.F., Speck, N.A., Peeters, M.C., and Dzierzak, E. (2000). Definitive hematopoietic stem cells first develop within the major arterial regions of the mouse embryo. EMBO J. 19, 2465–2474.

Espín, R., Roca, F.J., Candel, S., Sepulcre, M.P., González-Rosa, J.M., Alcaraz-Pérez, F., Meseguer, J., Cayuela, M.L., Mercader, N., and Mulero, V. (2013). TNF receptors regulate vascular homeostasis in zebrafish through a caspase-8, caspase-2 and P53 apoptotic program that bypasses caspase-3. Dis. Model. Mech. 6, 383–396.

Espinosa, L., Inglés-Esteve, J., Robert-Moreno, A., and Bigas, A. (2003). IkappaBalpha and p65 regulate the cytoplasmic shuttling of nuclear corepressors: cross-talk between Notch and NFkappaB pathways. Mol. Biol. Cell 14, 491–502.

Espinosa, L., Cathelin, S., D'Altri, T., Trimarchi, T., Statnikov, A., Guiu, J., Rodilla, V., Inglés-Esteve, J., Nomdedeu, J., Bellosillo, B., et al. (2010). The Notch/Hes1 pathway sustains NF-κB activation through CYLD repression in T cell leukemia. Cancer Cell 18, 268–281.

Faustman, D., and Davis, M. (2010). TNF receptor 2 pathway: drug target for autoimmune diseases. Nat. Rev. Drug Discov. 9, 482–493.

Fernandez, L., Rodriguez, S., Huang, H., Chora, A., Fernandes, J., Mumaw, C., Cruz, E., Pollok, K., Cristina, F., Price, J.E., et al. (2008). Tumor necrosis factor-alpha and endothelial cells modulate Notch signaling in the bone marrow microenvironment during inflammation. Exp. Hematol. 36, 545–558.

Gering, M., and Patient, R. (2005). Hedgehog signaling is required for adult blood stem cell formation in zebrafish embryos. Dev. Cell 8, 389–400.

Gerondakis, S., Banerjee, A., Grigoriadis, G., Vasanthakumar, A., Gugasyan, R., Sidwell, T., and Grumont, R.J. (2012). NF-κB subunit specificity in hemopoiesis. Immunol. Rev. 246, 272–285.

Godin, I., and Cumano, A. (2002). The hare and the tortoise: an embryonic haematopoietic race. Nat. Rev. Immunol. 2, 593–604.

Hadland, B.K., Huppert, S.S., Kanungo, J., Xue, Y., Jiang, R., Gridley, T., Conlon, R.A., Cheng, A.M., Kopan, R., and Longmore, G.D. (2004). A requirement for Notch1 distinguishes 2 phases of definitive hematopoiesis during development. Blood 104, 3097–3105.

Herbomel, P., Thisse, B., and Thisse, C. (1999). Ontogeny and behaviour of early macrophages in the zebrafish embryo. Development 126, 3735–3745.

Herbomel, P., Thisse, B., and Thisse, C. (2001). Zebrafish early macrophages colonize cephalic mesenchyme and developing brain, retina, and epidermis through a M-CSF receptor-dependent invasive process. Dev. Biol. 238, 274–288.

Johnston, D.A., Dong, B., and Hughes, C.C. (2009). TNF induction of jagged-1 in endothelial cells is NFkappaB-dependent. Gene 435, 36–44.

Kanther, M., Sun, X., Mühlbauer, M., Mackey, L.C., Flynn, E.J., 3rd, Bagnat, M., Jobin, C., and Rawls, J.F. (2011). Microbial colonization induces dynamic temporal and spatial patterns of NF-κB activation in the zebrafish digestive tract. Gastroenterology 141, 197–207.

Kim, A.D., Melick, C.H., Clements, W.K., Stachura, D.L., Distel, M., Panáková, D., MacRae, C., Mork, L.A., Crump, J.G., and Traver, D. (2014). Discrete Notch signaling requirements in the specification of hematopoietic stem cells. EMBO J. 33, 2363–2373.

King, K.Y., and Goodell, M.A. (2011). Inflammatory modulation of HSCs: viewing the HSC as a foundation for the immune response. Nat. Rev. Immunol. 11, 685–692.

Kissa, K., and Herbomel, P. (2010). Blood stem cells emerge from aortic endothelium by a novel type of cell transition. Nature 464, 112–115.

Kobayashi, I., Kobayashi-Sun, J., Kim, A.D., Pouget, C., Fujita, N., Suda, T., and Traver, D. (2014). Jam1a-Jam2a interactions regulate haematopoietic stem cell fate through Notch signalling. Nature 512, 319–323.

Kohchi, C., Noguchi, K., Tanabe, Y., Mizuno, D., and Soma, G. (1994). Constitutive expression of TNF-alpha and -beta genes in mouse embryo: roles of cytokines as regulator and effector on development. Int. J. Biochem. 26, 111–119.

Kondo, M., Wagers, A.J., Manz, M.G., Prohaska, S.S., Scherer, D.C., Beilhack, G.F., Shizuru, J.A., and Weissman, I.L. (2003). Biology of hematopoietic stem cells and progenitors: implications for clinical application. Annu. Rev. Immunol. 21, 759–806.

Kopan, R., and Ilagan, M.X. (2009). The canonical Notch signaling pathway: unfolding the activation mechanism. Cell 137, 216–233.

Kortschak, R.D., Tamme, R., and Lardelli, M. (2001). Evolutionary analysis of vertebrate Notch genes. Dev. Genes Evol. 211, 350–354.

Kumano, K., Chiba, S., Kunisato, A., Sata, M., Saito, T., Nakagami-Yamaguchi, E., Yamaguchi, T., Masuda, S., Shimizu, K., Takahashi, T., et al. (2003). Notch1 but not Notch2 is essential for generating hematopoietic stem cells from endothelial cells. Immunity 18, 699–711.

Kyba, M., and Daley, G.Q. (2003). Hematopoiesis from embryonic stem cells: lessons from and for ontogeny. Exp. Hematol. 31, 994–1006.

Lai, E.C. (2004). Notch signaling: control of cell communication and cell fate. Development 131, 965–973.

Langenau, D.M., Ferrando, A.A., Traver, D., Kutok, J.L., Hezel, J.P., Kanki, J.P., Zon, L.I., Look, A.T., and Trede, N.S. (2004). In vivo tracking of T cell development, ablation, and engraftment in transgenic zebrafish. Proc. Natl. Acad. Sci. USA 101, 7369–7374.

Lawson, N.D., Scheer, N., Pham, V.N., Kim, C.H., Chitnis, A.B., Campos-Ortega, J.A., and Weinstein, B.M. (2001). Notch signaling is required for arterial-venous differentiation during embryonic vascular development. Development 128, 3675–3683.

Le Guyader, D., Redd, M.J., Colucci-Guyon, E., Murayama, E., Kissa, K., Briolat, V., Mordelet, E., Zapata, A., Shinomiya, H., and Herbomel, P. (2008). Origins and unconventional behavior of neutrophils in developing zebrafish. Blood 111, 132–141.

Li, L., Jin, H., Xu, J., Shi, Y., and Wen, Z. (2011). Irf8 regulates macrophage versus neutrophil fate during zebrafish primitive myelopoiesis. Blood 117, 1359–1369.

Mizrahi, K., and Askenasy, N. (2014). Physiological functions of TNF family receptor/ligand interactions in hematopoiesis and transplantation. Blood 124, 176–183.

Parsons, M.J., Pisharath, H., Yusuff, S., Moore, J.C., Siekmann, A.F., Lawson, N., and Leach, S.D. (2009). Notch-responsive cells initiate the secondary transition in larval zebrafish pancreas. Mech. Dev. 126, 898–912.

Quillien, A., Moore, J.C., Shin, M., Siekmann, A.F., Smith, T., Pan, L., Moens, C.B., Parsons, M.J., and Lawson, N.D. (2014). Distinct Notch signaling outputs pattern the developing arterial system. Development 141, 1544–1552.

Rhodes, J., Hagen, A., Hsu, K., Deng, M., Liu, T.X., Look, A.T., and Kanki, J.P. (2005). Interplay of pu.1 and gata1 determines myelo-erythroid progenitor cell fate in zebrafish. Dev. Cell 8, 97–108.

Robert-Moreno, A., Guiu, J., Ruiz-Herguido, C., López, M.E., Inglés-Esteve, J., Riera, L., Tipping, A., Enver, T., Dzierzak, E., Gridley, T., et al. (2008). Impaired embryonic haematopoiesis yet normal arterial development in the absence of the Notch ligand Jagged1. EMBO J. 27, 1886–1895.

Roca, F.J., Mulero, I., López-Muñoz, A., Sepulcre, M.P., Renshaw, S.A., Meseguer, J., and Mulero, V. (2008). Evolution of the inflammatory response in vertebrates: fish TNF-alpha is a powerful activator of endothelial cells but hardly activates phagocytes. J. Immunol. 181, 5071–5081.

Sainson, R.C., Johnston, D.A., Chu, H.C., Holderfield, M.T., Nakatsu, M.N., Crampton, S.P., Davis, J., Conn, E., and Hughes, C.C. (2008). TNF primes endothelial cells for angiogenic sprouting by inducing a tip cell phenotype. Blood 111, 4997–5007.

Santoro, M.M., Samuel, T., Mitchell, T., Reed, J.C., and Stainer, D.Y. (2007). Birc2 (cIap1) regulates endothelial cell integrity and blood vessel homeostasis. Nat. Genet. 39, 1397–1402.

Cell

Shalaby, M.R., Sundan, A., Loetscher, H., Brockhaus, M., Lesslauer, W., and Espevik, T. (1990). Binding and regulation of cellular functions by monoclonal antibodies against human tumor necrosis factor receptors. J. Exp. Med. *172*, 1517–1520.

Shin, H.M., Minter, L.M., Cho, O.H., Gottipati, S., Fauq, A.H., Golde, T.E., Sonenshein, G.E., and Osborne, B.A. (2006). Notch1 augments NF-kappaB activity by facilitating its nuclear retention. EMBO J. *25*, 129–138.

Song, L.L., Peng, Y., Yun, J., Rizzo, P., Chaturvedi, V., Weijzen, S., Kast, W.M., Stone, P.J., Santos, L., Loredo, A., et al. (2008). Notch-1 associates with IKKalpha and regulates IKK activity in cervical cancer cells. Oncogene *27*, 5833–5844.

Stein, S.J., and Baldwin, A.S. (2013). Deletion of the NF-κB subunit p65/RelA in the hematopoietic compartment leads to defects in hematopoietic stem cell function. Blood *121*, 5015–5024.

Takizawa, H., Boettcher, S., and Manz, M.G. (2012). Demand-adapted regulation of early hematopoiesis in infection and inflammation. Blood *119*, 2991–3002.

Thisse, C., Thisse, B., Schilling, T.F., and Postlethwait, J.H. (1993). Structure of the zebrafish snail1 gene and its expression in wild-type, spadetail and no tail mutant embryos. Development *119*, 1203–1215.

van der Vaart, M., van Soest, J.J., Spaink, H.P., and Meijer, A.H. (2013). Functional analysis of a zebrafish myd88 mutant identifies key transcriptional components of the innate immune system. Dis. Model. Mech. *6*, 841–854.

Wang, H., Tian, Y., Wang, J., Phillips, K.L., Binch, A.L., Dunn, S., Cross, A., Chiverton, N., Zheng, Z., Shapiro, I.M., et al. (2013). Inflammatory cytokines induce NOTCH signaling in nucleus pulposus cells: implications in intervertebral disc degeneration. J. Biol. Chem. *288*, 16761–16774.

Westerfield, M. (2000). The Zebrafish Book. A guide for the laboratory use of zebrafish (Danio rerio), Fourth Edition (Eugene: Univ. of Oregon Press).

Wiens, G.D., and Glenney, G.W. (2011). Origin and evolution of TNF and TNF receptor superfamilies. Dev. Comp. Immunol. *35*, 1324–1335.

Wynn, T.A., Chawla, A., and Pollard, J.W. (2013). Macrophage biology in development, homeostasis and disease. Nature *496*, 445–455.

Zhao, C., Xiu, Y., Ashton, J., Xing, L., Morita, Y., Jordan, C.T., and Boyce, B.F. (2012). Noncanonical NF-κB signaling regulates hematopoietic stem cell self-renewal and microenvironment interactions. Stem Cells *30*, 709–718.

Zhao, J.L., Ma, C., O'Connell, R.M., Mehta, A., DiLoreto, R., Heath, J.R., and Baltimore, D. (2014). Conversion of danger signals into cytokine signals by hematopoietic stem and progenitor cells for regulation of stress-induced hematopoiesis. Cell Stem Cell *14*, 445–459.